

SOLAR ABSORBERS WITH A STRUCTURED SURFACE

JAN RIHACEK¹, MARTIN SARBORT², PETR HORNIK^{1,2}, LIBOR MRNA^{1,2}

¹Brno University of Technology, Faculty of Mechanical Engineering, Institute of Manufacturing Technology, Brno, Czech Republic

²Institute of Scientific Instruments of the Czech Academy of Sciences, Brno, Czech Republic

DOI: 10.17973/MMSJ.2018_06_2017102

e-mail: rihacek.j@fme.vutbr.cz

The article deals with the issue of a new type of solar absorbers, which have a direct flow structure and a structured surface, which consists of pyramidal cavities. This solution increases a thermal efficiency. In the first part, possible parameters that affect the thermal efficiency of solar collectors are described and further, a simulation of a dependence of a resulting absorption coefficient at a pyramidal apex angle and daytime or season is performed. For this purpose a simulation program was developed in the MATLAB software environment by using the Monte Carlo method. The second part of the paper deals with the possibilities of production of the solar absorber with the structured surface, mainly by using the pillow hydroforming technology. The production process is simulated in ANSYS software. In this case, an austenitic chromium nickel stainless steel X5CrNi18-10 is used as a material for the production of solar absorbers.

KEYWORDS

solar absorber, numeric simulation, hydroforming, X5CrNi18-10 steel, MATLAB, ANSYS, LS-DYNA

1 INTRODUCTION

Thermal solar collectors absorb sunlight and convert it into a heat that is transferred to the heat exchange fluid for further use, such as DHW heating, pool water heating, and absorption cooling systems. When designing them, of course, there is an effort to maximize a thermal gain from solar radiation. Flat plate solar collectors are relatively simple in their production and therefore economical. On the other hand, they are unable to reach the maximum heat gain during the year because they are fixed. However, the sun moves through the sky in so-called daily and annual path. The impact of solar radiation is therefore not perpendicular considering absorption surface, but the perpendicular incidence is necessary for the maximal absorption. Systems of active routing of solar collectors would cost the overall investment so much that the whole system would not be economically profitable. Nowadays there are possibilities to solve this problem, for example a transparent cover plate of the collector with scattering elements. However, this option increases the overall optical loss of radiation through the scattering plate.

Another way is to make the flat plate solar absorber with the structured surface. The structure consists of pyramidal cavities inside which the solar radiation will be absorbed by multiple reflections. The expected benefits of this solution are two: firstly, this arrangement will increase the cumulative surface absorbance and secondly, it should decrease (by passive path) the dependence on the sun's running. [Duffie 2013]

2 SIMULATION OF A CUMULATIVE ABSORPTION AND AN ENERGY GAIN OF THE SOLAR ABSORBER

The basic parameter of the pyramid is its apex angle α . A parallel flow of the solar radiation, which is partially absorbed and partially reflected, strikes the pyramidal cavity. Due to the daily and annual sun path, the incident radiation changes the angle of impact into the cavity, which complicates the situation. [Duffie 2013], [Abood 2015]

The problem cannot be solved analytically - using an equation, but it must be simulated. For the study of the radiation absorption, a program was developed in the MATLAB software environment. The Monte Carlo method was chosen for the calculation when a light beam was randomly released into the studied pyramid. This beam is reflected between the individual walls of the pyramid by using Raytracing method. With a sufficient number of released rays, we will achieve a representative and steady state results in terms of the average number of reflections and overall absorption. The whole program is quite complex with the requirement of the following parameters:

- apex angle α of the pyramidal cavity,
- collector inclination relative to the horizontal plane (slope angle β),
- collector angle of rotation relative to the south (azimuth angle Z),
- absorbance A of the collector surface (dependence of the absorbance on the incidence angle),
- geographical latitude L and height above sea level h (we used Brno coordinates $L = 49.191^\circ \text{ N}$, $h = 259 \text{ m}$),
- daily sunshine (for a specific geographic position, cloud effect is not considered),
- sun's annual path (for a specific geographic position).

These parameters affect the number of reflections inside the cavity and thus the amount of absorbed radiation. At first, a simulation of the resulting cumulative absorbance A_c for normal incidence at the top of the pyramid was performed.

Results of the simulation, of course, depend on the total average number of reflections for a particular apex angle, see Fig. 1 and Fig. 2.

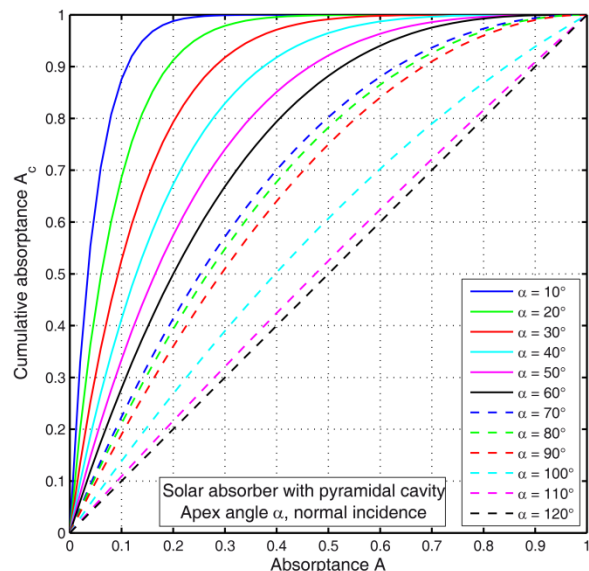


Figure 1. Cumulative absorbance depending on the apex angle of the pyramid

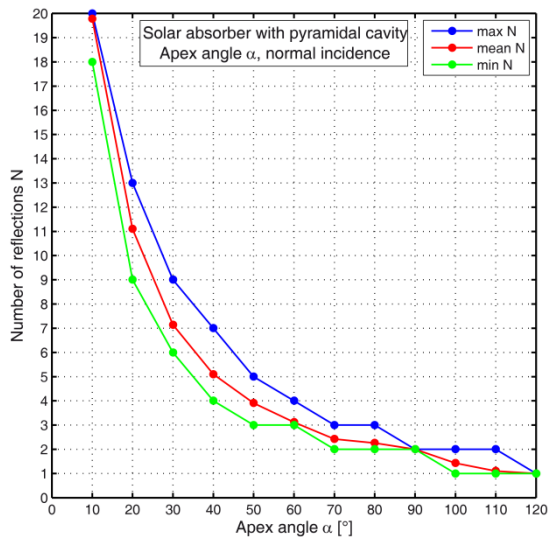


Figure 2. The number of reflections inside the pyramid depending on the pyramid's apex angle

It is evident that the cumulative absorptance increases with a narrowing pyramid – this corresponds to an increasing number of reflections within the pyramid. On the other hand, in terms of a sheet metal forming technology, it is not possible to form a surface with too narrow and deep pyramids. Therefore, for theoretical simulations as well as practical experiments, pyramids with the apex angle of 90° and 60° were selected. In the first case, there are on average two reflections in the pyramid, in the second case, there are three reflections. In the real situation, however, the perpendicular impact of solar radiation on the plane of the solar absorber does not always occur. Other dependencies are therefore modeled for four typical days of the year:

- winter solstice – minimum length of sunshine, minimum sunshine over the horizon,
- spring and autumn equinox (the same day path of the sun),
- summer solstice – maximum sunshine, maximum noon sunrise above the horizon.

The following three graphs (Fig. 3, Fig. 4 and Fig. 5) show a change in the cumulative absorptance depending on the daytime path of the sun for the aforementioned days. Low surface absorptance $A = 0.2$ was chosen to make a well-evident dependence of the cumulative absorptance on the daytime sunrise for different apex angles of the pyramids.

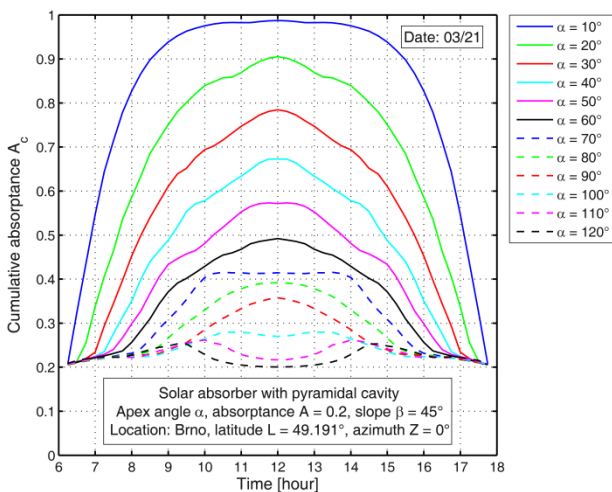


Figure 3. Cumulative absorptance for the spring and autumn equinox

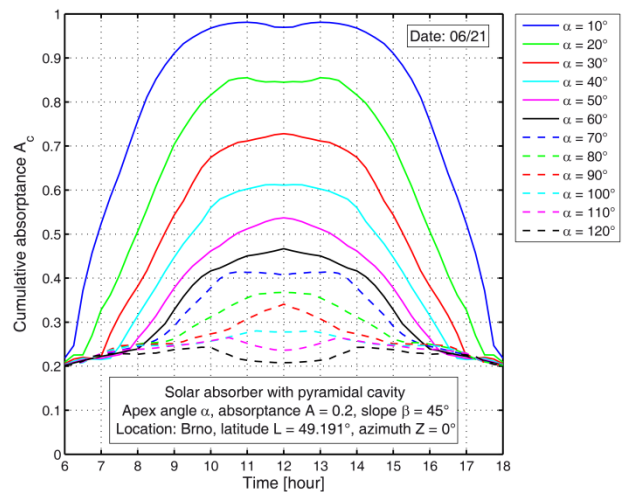


Figure 4. Cumulative absorptance for the summer solstice

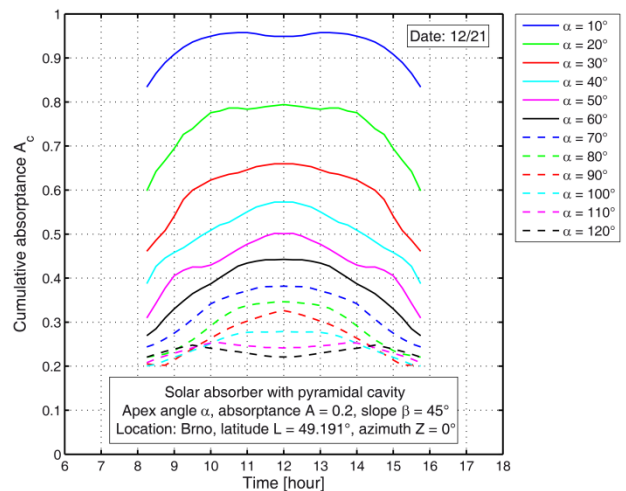


Figure 5. Cumulative absorptance for the winter solstice

It is clear from the simulations that cumulative absorptance dependence is not trivial smooth curve, but it has a complex course. In all cases, there is an increase in cumulative absorptance which culminates during the day and then drops again. For additional simulations, it is necessary to define several variables:

- Absorptance (cumulative) A_c – cumulative fraction of incident light power that is absorbed due to multiple reflections,
- Cosine factor $\cos \theta$ – cosine correction due to the angle θ between light ray and normal vector to the absorber plane,
- Solar constant I_s – solar irradiance constant above Earth's atmosphere ($I_s = 1367 \text{ W} \cdot \text{m}^{-2}$),
- Air mass coefficient AM – ratio of direct optical path length through Earth's atmosphere to zenith optical path length (standardized value $AM = 1.5$ was used [Kasten 1989])
- Irradiance I – direct solar irradiance at the Earth's surface

$$I = I_s \cdot \left[\left(1 - \frac{h}{7.1} \right) \cdot 0.7^{(AM)^{0.678}} + \frac{h}{7.1} \right] [W] \quad (1)$$

where the height above sea level h is given in km [Laue 1970] (the diffuse component of light is not considered)

- Radiant power (cumulative) P_c – cumulative radiant flux – cumulative radiant energy received per unit time, relative to the surface S , defined as:

$$P_c = I \cdot A_c \cdot S \cdot \cos \theta [W] \quad (2)$$

- Radiant exposure (reference) H – radiant energy received by a surface per unit area, or equivalently irradiance of a surface integrated over time of irradiation defined as:

$$H = \int I \cdot A_c \cdot \cos \theta \cdot dt [J \cdot \text{m}^{-2}] \quad (3)$$

- Radiant exposure (cumulative) H_c – cumulative radiant energy received by a surface per unit area, or equivalently cumulative irradiance of a surface integrated over time of irradiation defined as:

$$H_c = \int I \cdot A_c \cdot \cos \theta \cdot dt \quad [J \cdot m^{-2}] \quad (4)$$

- Radiant energy (reference) E – energy of absorbed electromagnetic radiation defined as:

$$E = \int I \cdot A \cdot S \cdot \cos \theta \cdot dt = H \cdot S \quad [J] \quad (5)$$

- Radiant energy (cumulative) E_c – energy of absorbed electromagnetic radiation defined as:

$$E_c = \int I \cdot A_c \cdot S \cdot \cos \theta \cdot dt = H_c \cdot S \quad [J] \quad (6)$$

- Efficiency (reference) η – efficiency of reference solar absorber (flat surface, single reflection), ratio of reference and ideal radiant exposure defined as:

$$\eta = \frac{H}{H_i} \quad (7)$$

- Efficiency (cumulative) η_c – cumulative efficiency of solar absorber with pyramidal cavities (multiple reflections), ratio of cumulative and ideal radiant exposure defined as:

$$\eta_c = \frac{H_c}{H_i} \quad (8)$$

Based on these calculations, an efficiency and power gain simulation was performed for the 60° and 90° apex angles for the orientation of the solar collector to the south and various angles of slope from horizontal to vertical. The results are always compared with the reference solar collector, which has the planar absorption surface, see Fig. 6 and Fig. 7.

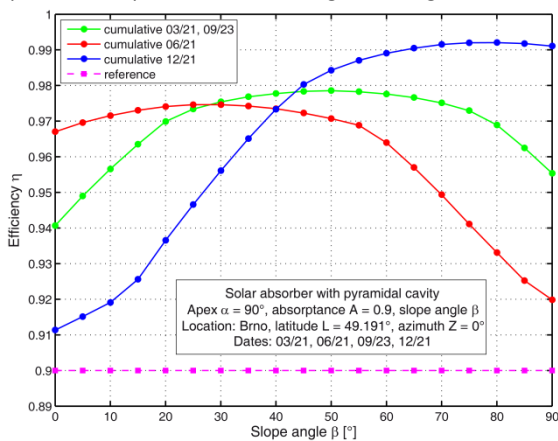


Figure 6. Cumulative efficiency of solar absorber with the 60° pyramids for different slope angle. Absorber heading south. Calculation for three characteristic days of the year.

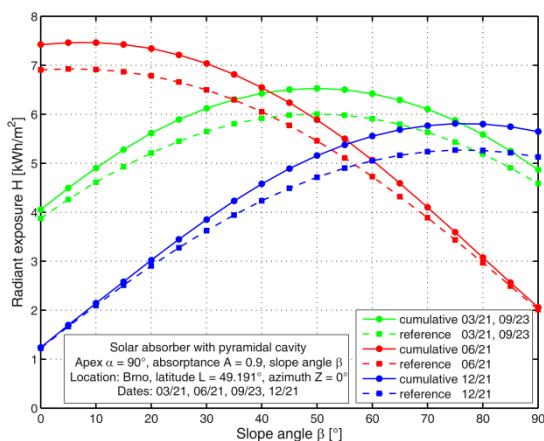


Figure 7. Received heat for the absorber with the 60° pyramids for different slope angle. Absorber heading south. Calculation for three characteristic days of the year. The reference is a flat absorber.

The energy gain graph shows energy benefits against a flat absorber. How it is clear from the graphs, the efficiency and the energy gain differ for a specific slope in different seasons and it will be necessary to choose a compromise angle that will maximize the total energy gain for the whole year. An angle of 45° was chosen. For this angle, the efficiency was calculated for all days of the year and in the same way the energy gain during the year was calculated too.

By integrating this curve, a total annual energy of 1m² of the solar collector surface was obtained, i.e. for the pyramids apex angles of 60°, 90° and 180° - the flat plate (reference) absorber. The results are shown in Fig. 8 and Fig. 9.

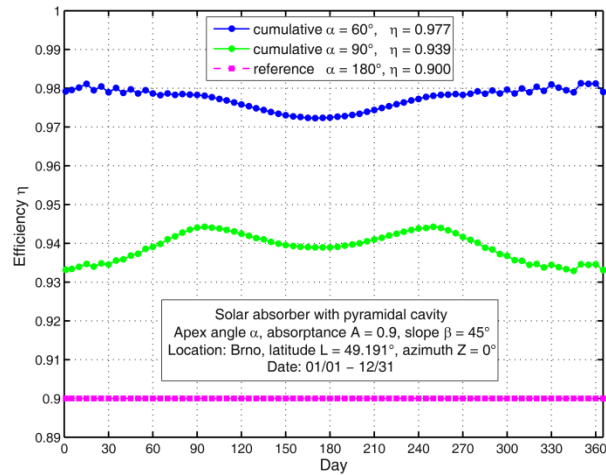


Figure 8. Cumulative efficiency of solar absorbers surface for three pyramidal apexes during the year, slope angle is 45°, absorber heading south.

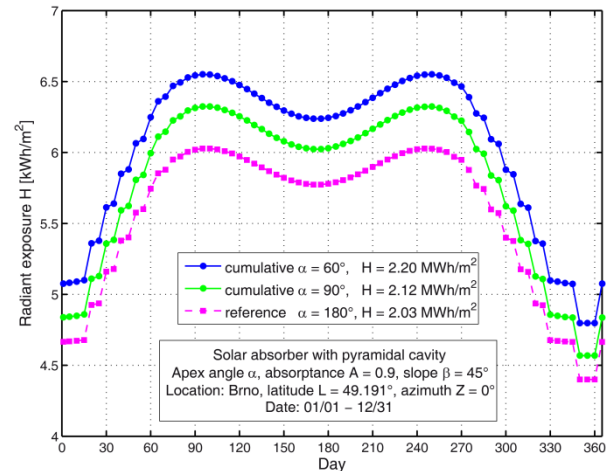


Figure 9. Total annual energy of 1m² of the solar collector surface for three pyramidal apexes during the year, slope angle is 45°, absorber heading south.

From simulations, following conclusions can be made:

- the efficiency of the solar collector with the structured surface is higher for the chosen 90° and 60° apex angles compared to the reference planar surface,
- during the year, the efficiency fluctuates within about 8 %,
- similarly, the energy yield fluctuates over the year, due to different times of sunshine and the effect of the different daytime sun path,
- if we compare the integrals of the obtained energy efficiency curves, then for the angle of inclination, the total energy contribution of the structured surface with the apex angle 90° is 4.4% higher, the annual energy contribution is 8.8% higher for the structured surface with the apex angle of 60°,

- the simulation results reveal primarily on the effect of the structured surface, since the following assumptions were made – we assumed the day's maximum sunshine without the cloud effect, we chose a constant air mass coefficient and we neglected the diffuse component of the solar irradiance,
- simulations have shown that the solar collector with the structured surface has a positive effect on the overall energy efficiency and this benefit increases with decreasing of the apex angle of the pyramids, i.e. it makes sense to deal with the technology of production of the structured surface.

Open question is the dependence of absorption on the angle of radiation impact. It is known that this magnitude depends on surface roughness, wavelength and other factors. Including these factors in the calculation would lead to further refinement of the simulation and will be carried out in the next stage.

3 PRODUCTION TECHNOLOGY OF SOLAR ABSORBERS WITH THE STRUCTURED SURFACE

Furthermore, the manufacturing of the pyramidal structure have to be considered. It is clear that the limitations of production technologies do not allow the production of the pyramidal structure with any apex angles, i.e. too narrow and deep pyramids. Therefore, as it was mentioned before, the theoretical and practical study of the manufacturability was focused on the pyramidal structure with the apex angle of 90° and 60°. The main requirements for the absorber material are, among other things, good weldability, formability and thermal conductivity. These requirements are met by X5CrNi18-10 austenitic chromium nickel stainless steel which was chosen as the blank material. Basic properties of the steel are given in Tab. 1.

Tensile modulus	E	[MPa]	$1.99 \cdot 10^5$
Yield strength	$R_{p0.2}$	[MPa]	291
Ultimate strength	R_m	[MPa]	700
Ductility	A_5	[%]	50
Density at 20 °C	ρ	[kg·m ⁻³]	$7.9 \cdot 10^3$
Specific heat capacity	c_p	[J·kg ⁻¹ ·K ⁻¹]	500
Thermal conductivity at 20 °C	λ_t	[W·m ⁻¹ ·K ⁻¹]	14,7

Table 1. Main properties of X5CrNi18-10 steel

The main technology involved in the production is the pillow hydroforming method. In a principle, two sheet blanks, which are mostly welded around the circumference, are placed into the tool. Circumferential welding ensures that the system is tight and that the plates are correctly positioned against each other. After clamping of an upper and a lower die of the tool, a pressure liquid is introduced into a gap between sheets, which starts to form them, see Fig. 10. [Hosford 2014], [Koc 2008]

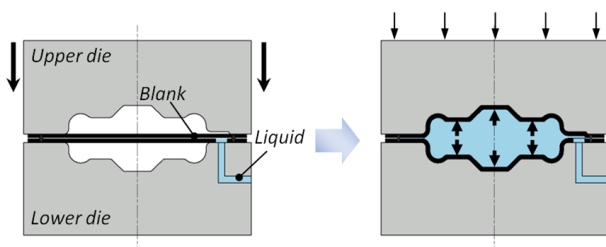


Figure 10. Principle of the pillow hydroforming method

However, the entire production process of the solar absorber with the structured surface consists of several stages, according to Fig. 11:

1. production of two sheet blanks by laser cutting technology (considered thickness of sheets is 0.5 mm to 1.0 mm),
2. creating of two holes with threads in one of these sheets by thermal drilling technology (Flowdrill method) as input and output for forming and heat exchange liquid,
3. welding two sheet blanks together by penetration laser welding, creating of a meandering structure for better heat transfer fluid flow and creating of spot welds (circular welds) to increase the absorber stiffness,
4. forming (hydroforming) of the weldment in the hydroforming tool,
5. possible coating of the absorber to increase its thermal efficiency.

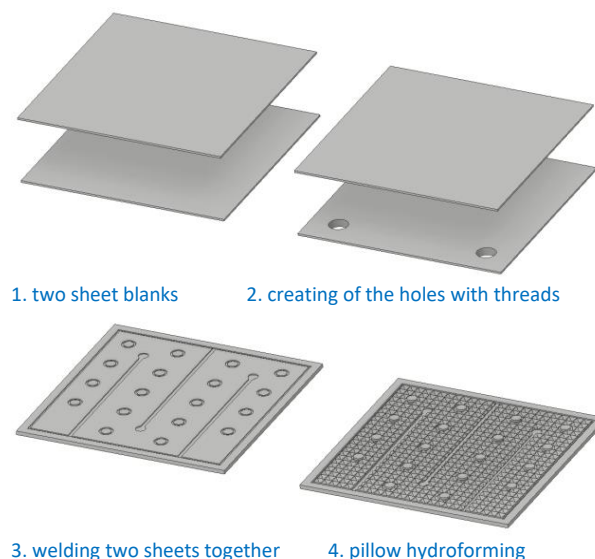


Figure 11. Production process of the solar absorber

The solution to the problem with creating of the structured surfaces by the hydroforming, as well as the welding process, must first be verified on a sample with smaller dimensions. Therefore, the sample with dimensions of 250 x 250 mm was firstly considered for realization of the structured surface, before the forming of the structured surface over the entire absorber surface (1000 x 1000 mm). A simplified variant of the meandering structure (central weld) was created in the sample. The sample was welded from two sheets: the base sheet with inlet and outlet of the forming medium has a thickness of 1 mm and the formed sheet is 0.5 mm or 0.8 mm thick, according to the apex angle of structured surface pyramids. For verification of the forming process, the hydroforming device was developed which uses the cassette system, see the schematic design in Fig. 12. [Mrna 2015]

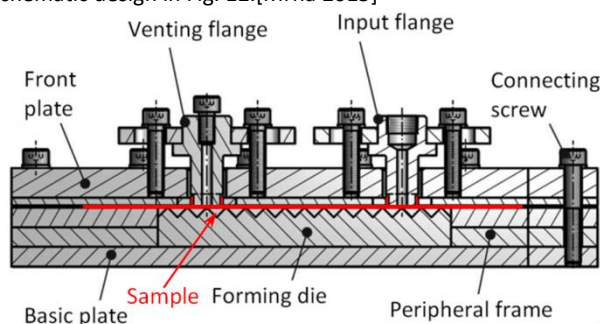


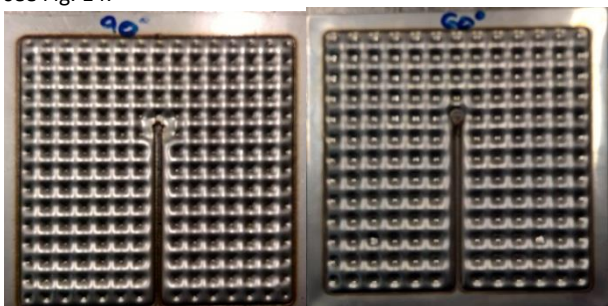
Figure 12. Hydroforming device – cross section [Mrna 2015]

The hydroforming process performs here in a high-pressure cassette with an inner die surface corresponding to the desired structured surface of the absorber. In order to test a different geometry of pyramidal cavities, the construction of the device is adapted to readily replace of the forming die, which creates the structured surface. A pressure of the forming medium (HM-46 oil) is controlled via a two-stage manual pressure pump with a maximum pressure of 70 MPa, which is connected to the device by a quick screw connector. The inlet of the forming liquid into the sample is realized via the hemmed hole with G1/4" thread, into which the screw connector is screwed. Device components are made of a S235JRG2 structural steel plates with thickness of 15 mm. The resulting load during the forming operation would cause the die swelling. Therefore, the device is supported by using a hydraulic press (CBJ 500-6), which applies a counterforce to the forming pressure of the hydraulic oil, see Fig. 13.



Figure 13. Hydroforming device in a hydraulic press

Thanks to this solution, the first experimental samples of the structured surface with 60° and 90° apex angles were formed, see Fig. 14.



a) apex angle of 90° b) apex angle of 60°

Figure 14. Formed structure surface

However, in the case of hydroforming, there are often defects, namely cracks in the area of the weld-formed material near the center weld and cracking at the top of the pyramidal shape. Therefore, it is necessary to optimize the hydroforming process by using the numerical simulation.

4 SIMULATION OF THE HYDROFORMING PROCESS

The simulation solution of the hydroforming process uses the finite element method. For this purpose, LS-DYNA software was used in cooperation with ANSYS Workbench software.

4.1 Material model

Firstly, a hardening curve of the formed material (X5CrNi18-10) was determined for the rolling direction, which was then converted to the coordinates of true stress-true strain curve, see Fig. 15.

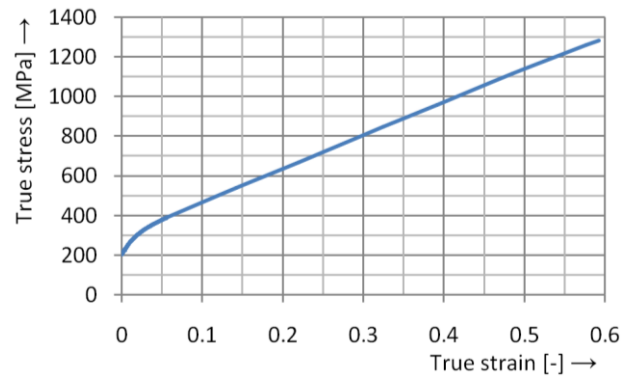


Figure 15. Stress-strain curve of X5CrNi18-10 Steel

Furthermore, an anisotropic effect of the X5CrNi18-10 steel was determined by performing tensile tests in different directions relative to the rolling direction (0°, 45° and 90°) for 20 % of the plastic strain.

Coefficients of a normal anisotropy were determined according to the equation (8) as $r_0 = 0,865$, $r_{45} = 1,174$, $r_{90} = 0,972$.

$$r_\alpha = \frac{\varphi_b}{\varphi_s} = \frac{\ln \frac{b_0}{b}}{\ln \frac{s_0}{s}} \quad (9)$$

where φ_b is true strain in the direction of the width of the specimen, φ_s is true strain in the direction of the thickness of the specimen, b_0 is the initial width of the specimen, s_0 is the initial thickness of the specimen, b is the final width of the specimen and s is the final thickness of the specimen.

Changing of the normal anisotropy coefficient for different directions relative to the rolling direction shows Fig. 16.

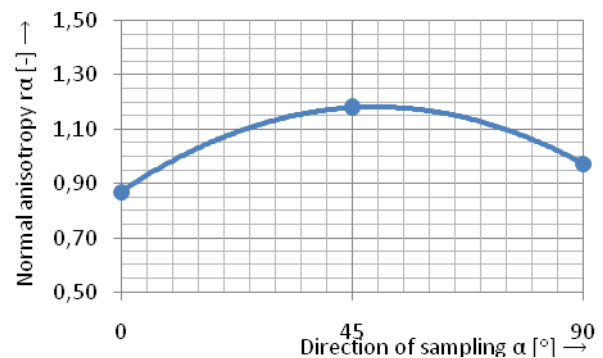


Figure 16. Dependence of normal anisotropy coefficient on the direction of sampling

4.2 Geometrical Model

The geometric model uses a half symmetry. It can also be simplified by neglecting parts of the geometry that do not affect the forming process. The geometric model of the simulation including used supports is shown in Fig. 17.

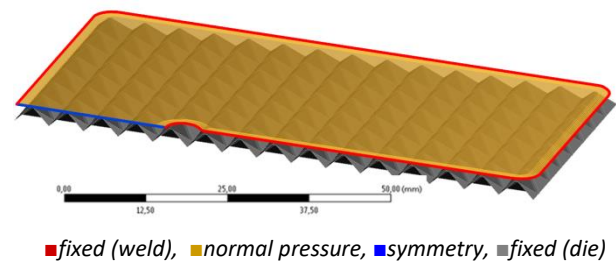
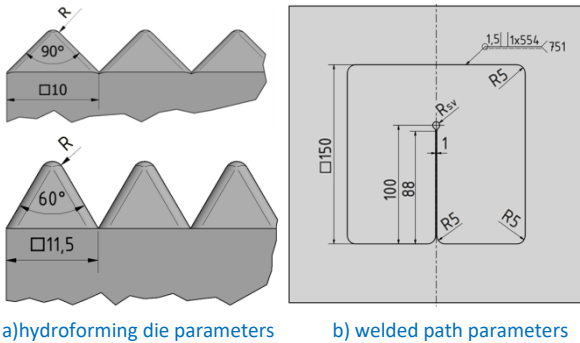


Figure 17. Geometrical model

4.3 Results

The numerical simulation by using LS-DYNA software gives a stamping depth and required pressure as a primary results. However, for the optimization of the forming process, it is important to determine the geometry of the center weld (R_{sv} radius) and the optimal shape of the structured surface pyramids (radius of die edges – R) according to Fig. 18.



a) hydroforming die parameters b) welded path parameters

Figure 18. Geometrical model

In the first step, the simulation achieved the optimal dimensions of the hydroforming die, i.e. die radius R, and forming pressure p according to Fig. 18a. The evaluation was performed for both apex angles (90° and 60°).

For apex angle of 90°, optimal parameters were found as $R = 1 \text{ mm}$ and $p = 70 \text{ MPa}$ for the initial sheet thickness of 0.5 mm . Values are based on the dependence between the stamping depth h, the die radius R and the forming pressure p from the 3D contour graph in Fig. 19.

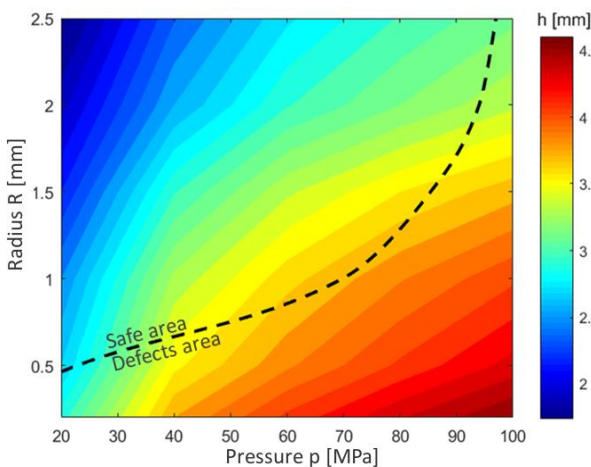


Figure 19. R-p-h graph for thickness of 0.5 mm and the angle of 90°

In the case of the 60° apex angle, a greater thickness of 0.8 mm has to be considered. In the other cases, the sheet is formable only to a very small depth. For the thickness of 0.8 mm and the angle of 60°, the following optimal parameters were found: the die radius $R = 2 \text{ mm}$ and the forming pressure $p = 65 \text{ MPa}$, see Fig. 20.

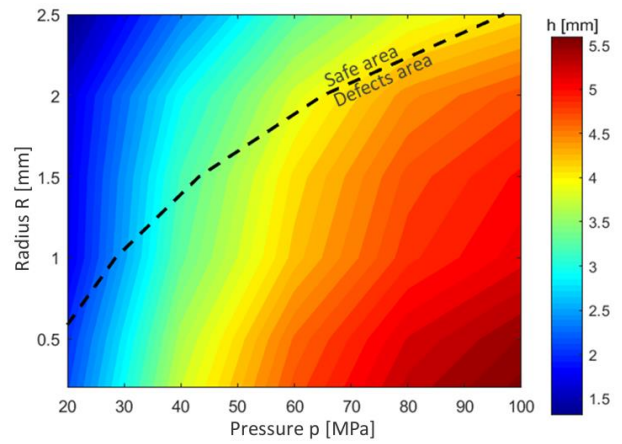


Figure 20. R-p-h graph for thickness of 0.8 mm and the angle of 60°

The determination of optimal parameters of the central weld were next results. For both cases (90° and 60° angles), results are almost identical. The most effective seems to be a "drop-shaped" end with radius $R_{sv} = 3 \text{ mm}$. This value is based on the graph in Fig. 21. Graph represents the dependence between major true strains ratio of the material in the welded area, the forming pressure and the rounding radius. The safe area was determined by using forming limit diagram (FLD) for the X5CrNi18-10 steel, i.e. the permitted major true strains ratio, see Fig. 22, which shows an example of true strain points distribution in the FLD for the forming pressure of 65 MPa.

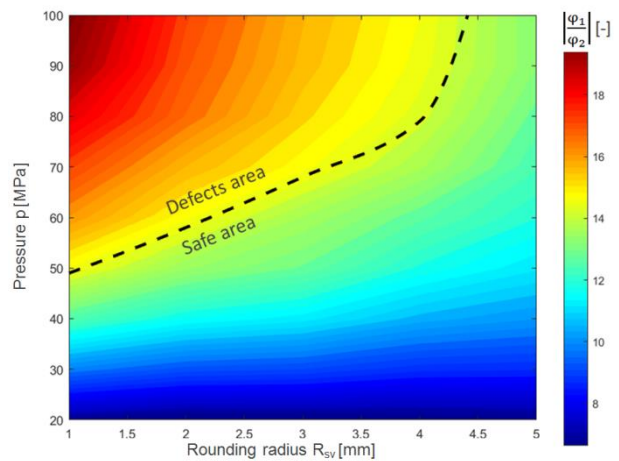


Figure 21. $\frac{\phi_1}{\phi_2}$ -p- R_{sv} 3D graph for thickness of 0.8 mm and the 60° angle

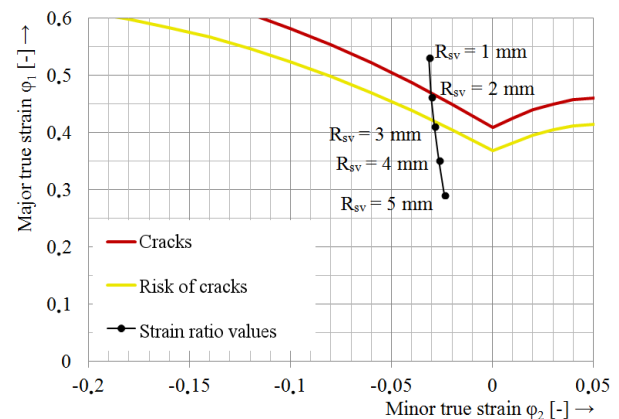


Figure 22. Point positions in FLD at $p = 65 \text{ MPa}$

5 CONCLUSIONS

Based on the main drawbacks of flat plate solar absorbers, the new concept of the solar absorber was proposed, where the meandering structure created throughout the whole absorber area combined with the structured surface in the form of pyramidal cavities enable increase absorption of solar radiation and also the higher absorber efficiency (compared to a flat absorber of 6-9%).

Simulations of the dependence of the cumulative absorption at the pyramidal apex angle and simulation of the cumulative absorption change as a function of the daytime sun path were performed in MATLAB software. Simulations have shown that the solar collector with the structured surface has a positive effect on the overall energy efficiency.

Furthermore, the technology of the production for the proposed type of the solar absorber was designed. The structured surface with pyramidal apex angles of 90° and 60° was considered. For verification of the production process of the absorber with the structured surface, the hydroforming device was designed and implemented. Practical tests with the sample, which is made of X5CrNi18-10 steel, were performed. At the same time, the production of the structured surface by the hydroforming technology was simulated in LS-DYNA software. Thanks to simulations, limit values of forming pressure, the die radius and optimal dimensions of the central weld for the formed sample were found.

ACKNOWLEDGMENTS

The contribution was supported by TA CR project: "Development of new types of solar absorbers" no. TA04020456 and with the support of the European Commission and the Ministry of Education Youth and Sports of the Czech Republic (project no. CZ.1.05/2.1.00/01.0017) and NPU LO1212.

REFERENCES

- [Abood 2015] Abood, A. A. A comprehensive solar angles simulation and calculation using Matlab. *International Journal Energy & Environment*, 2015, Vol.6, pp 367-376, ISSN 2076-2909
- [Duffie2013] Duffie, J. A. and Beckman, W. A. *Solar Engineering of Thermal Processes*. Hoboken: John Wiley, 2013. ISBN 978-0-470-87366-3
- [Hosford 2014] Hosford, W. F. and Caddel, R. M. *Metal Forming: Mechanics and Metallurgy*. Cambridge: Cambridge University Press, 2014. ISBN978-1-107-00452-8

[Kasten 1989] Kasten, F. and Young, A. T. Revised optical air mass tables and approximation formula. *Applied Optics*, 1989, Vol.28, pp 4735–4738, ISSN

[Koc 2008] Koc, M. *Hydroforming for Advanced Manufacturing*. Cambridge: Woodhead Publishing, 2008. ISBN978-1-84569-328-2

[Laue 1970] Laue, E. G. The measurement of solar spectral irradiance at different terrestrial elevations. *Solar Energy*, 1970, Vol. 13, pp 43-50, IN1-IN4, 51-57.

[Mrna 2015] Mrna, L. and Rihacek, J. Forming a Structured Surface of a New Type of Solar Absorber with Hydroforming. *Advanced Materials Research*, 2015, Vol.1127, pp 49-53, ISSN 1022- 6680

CONTACTS:

Ing. Jan Rihacek, Ph.D.
Brno University of Technology
Faculty of Mechanical Engineering,
Institute of Manufacturing Technology, Department of Metal Forming
Technicka 2896/2, Brno, 616 69, Czech Republic
e-mail: rihacek.j@fme.vutbr.cz

Mgr. Martin Sarbort, Ph.D.
Institute of Scientific Instruments of the Czech Academy of Sciences
Kralovopolska 147, Brno, 612 64, Czech Republic
e-mail: martins@isibrno.cz

doc. RNDr. Libor Mrna, Ph.D.
Institute of Scientific Instruments of the Czech Academy of Sciences
Kralovopolska 147, Brno, 612 64, Czech Republic
e-mail: mrna@isibrno.cz
Brno University of Technology, Faculty of Mechanical Engineering, Institute of Manufacturing Technology, Department of Welding and Surface Treatment
Technicka 2896/2, Brno, 616 69, Czech Republic
e-mail: mrna@fme.vutbr.cz

Ing. Petr Hornik
Institute of Scientific Instruments of the Czech Academy of Sciences
Kralovopolska 147, Brno, 612 64, Czech Republic
e-mail: hornik@isibrno.cz